The Mass Attenuation Coefficients and Effective Atomic Numbers of Y-Based Superconductors in Energy Range 220 keV to 662 keV

Thitipong Kruaehong [a, *], Wuttichai Chaiphaksa [b], Jakrapong Kaewkhao [b], Supphadate Sujinnapram [c], Pongkaew Udomsamuthirun [d, e]

[a] *Department of Physics, Faculty of Science and Technology, Suratthani Rajabhat University, Surat Thani, 84100 Thailand*
[b] *Science Program, Faculty of Science and Technology, Nakhon Pathom Rajabhat University, Nakhon Pathom, 73000 Thailand*
[c] *Department of Physics, Faculty of Liberal Arts and Science, Kasetsart University, Kamphaeng Saen Campus, Nakhon Pathom, 73140 Thailand*
[d] *Prasarnmit Physics Research Unit, Department of Physics, Faculty of Science, Srinakharinwirot University, Bangkok, 10110 Thailand*
[e] *Thailand Center of Excellence in Physics (ThEP), Si Ayutthaya Road, Bangkok, 10400 Thailand*

Received 19 June 2019; Revised 16 August 2019; Accepted 20 August 2019

Abstract

The mass attenuation coefficients and effective atomic numbers of the new Y-based superconductors have been studied in the energy range of 220 – 662 keV. The variation of photon energy has been changed from Cs-137 (662 keV) by Compton scattering technique. The mass attenuation coefficients of Y-based superconductors decreased with increasing of photon energy and do not show the significantly different compared with all Y-based superconductors. Incoherent scattering is main interaction process when photon penetration to Y-based superconductors. The effective atomic numbers and electron densities show the same trend and its depend on Y, Ba and Cu content in Y-based superconductors.

KEYWORDS: Y-based superconductors; Solid state reaction; Mass measurement

*Corresponding authors; e-mail: kruaehong@hotmail.com

Introduction

In 1986, Bednorz and Muller [1] reported that the metal oxide ceramic $La_{2-x}Ba_xCuO_4$(La214) becomes superconducting above 30 K. The superconductivity of La214 initiated a flurry of research on a new family materials referred to as high-temperature superconductors. The Y123($YBa_2Cu_3O_y$) was the first discovered by Chu and co-workers [2] in 1987 with the critical temperature transition around 93 K. The other Y-based superconductors discovered in 1988 were two groups of Y124($YBa_2Cu_4O_8$) and Y247($Y_2Ba_4Cu_7O_{15}$). The critical temperatures of Y124 [3] and Y247 [4] were 80 K and 40 K, respectively. The Y247 have various critical temperature values depend on the oxygen content [5]. The Y247 showed critical temperature interval 30 K to 95 K. In 2009, Alibadi et al [6], synthesized the new compound of the Y-based superconductors in Y358($Y_3Ba_5Cu_8O_{18}$) with the highest critical temperature in YBaCuO family at 102 K prepared by the solid state reaction method. The model of Y358 structure was simulated by Tavana and Akhavan [7] in 2010. The crystal structure features of Y358 are similarly with Y123 superconductor. The *a* and *b* lattice parameters of Y358 are closely Y123 excluding *c* lattice parameters. The *c* lattice parameters of Y358 were increased more than 3 times of Y123. Recently, Udomsamuthirun et al [8] used the assumption that the number of Y-atoms plus Ba-atoms was equal Cu-atoms synthesized the new Y-based superconductors. The formulas of new Y-based were Y156, Y3-8-11, Y5-6-11, Y5-8-13, Y7-11-18, Y7-9-16, Y13-20-33 which synthesized by solid state reaction. The critical temperature values of the bulk samples were characterized by the four-probe resistivity measurement. Their resulted, The Y3-8-11 show the sharp transition critical temperature and has highest onset critical

temperature at 94 K. From the XRD result of Y358 [7], The *c* lattice parameters of Y358 was increased more than Y123 about 19.4799 Å. In 2010, Sujinnapram et al [9] take the raw data of XRD in the new approach analyzed method with the Rietveld refinement method [10] for determined the lattice parameter of superconducting compound and non-superconducting compound and space group. The superconducting compound has orthorhombic structure with Pmmm space group. The non-superconducting compound has various crystal structure and space group. The superconducting compound results reveal that the new Y-based superconductors have *a* and *b* lattice parameter closely in *a* and *b* lattice parameter of Y123, but the *c* lattice parameters were increasing with Cu-atoms. The non-superconducting compound was no effect increasing in *c* lattice parameter. The graph plot between *c* lattice parameter versus Cu-atoms was linear curve [9]. Therefore, The research in Y-based superconductors was most attraction. The discovery of Y-based superconductors have many researchers [11 – 15] and improve the physical properties for application whether the high critical currentdensity (J_c) [16], high critical magnetic field (H_c) [17], mechanical [18], microstructure [19] and magnetic application such as the maglev train [20], the magnetic bearing [21], the flywheel energystorage [22], and the trapped flux magnet [23].

The superconducting materials are expected to constitute most electric circuits in the near future. Some of these circuits may be exposed to radiation as in nuclear reactors, satellites, nuclear weapons, nuclear medicine. So that the knowledge of the absorption of gamma radiations in superconducting materials will be prime important. The mass attenuation coefficients and effective atomic number are basic quantity required for determining the attenuation of X-rays and gamma-rays in matter and is potentially useful in the development of semi-empirical formulations of high accuracy. Most of previous measurements of mass attenuation coefficients and effective atomic numbers have been performed on many materials in many applications such as concrete [24 – 26], alloys [27 – 30], stainless steel [31], gemstones [32 – 33], glasses [34 – 39], polymer [40 – 41] and superconductors [42 – 44]. These observations have been compared with theoretical values calculated from WinX Com program [45 – 46].

In this work, the mass attenuation coefficients and the effective atomic numbers of Y123, Y358 and Y3-8-11 superconductors were measured in the photon energy range 220 – 662 keV. The variation of photon energy have been changed from Cs-137 (662 keV) by Compton scattering technique.

The mass attenuation coefficient and effective atomic number

The mass attenuation coefficient is written as [34]

$$\mu_m = \frac{\ln(I_0/I)}{\rho t} \tag{1}$$

where ρ is the density of material (g cm^{-3}), I_0 and I are the incident and transmitted intensities and t is the thickness of absorber (cm).

Theoretical values of the mass attenuation coefficients of mixture or compound have been calculated by WinX Com, base on mixture rule [45 – 46]

$$\mu_m = \sum_i w_i (\mu_m)_i \tag{2}$$

where w_i weight fraction of each element in mixture, $(\mu_m)_i$ is mass attenuation coefficient for individual element in mixture. The value of mass attenuation coefficients can be used to determine the total atomic cross-section ($\sigma_{t,a}$) by the following relation [34]

$$\sigma_{t,a} = \frac{(\mu_m)_{alloy}}{N_A \sum_i^n (w_i / A_i)} \tag{3}$$

Where N_A is Avogradro's number, A_i is atomic weight of constituent element of mixture. Also the total electronic cross-section ($\sigma_{t,el}$) for the element is expressed by the following formula [34]

$$\sigma_{t,el} = \frac{1}{N_A} \sum_i^n \frac{f_i A_i}{Z_i} (\mu_m)_i \tag{4}$$

Where f_i is the number of atoms of element *i* relative to the total number of atoms of all elements in alloy, Z_i is the atomic number of the i^{th} element in mixture. Total atomic cross-section and total electronic cross-section are related to effective atomic number (Z_{eff}) of the compound through the formula [34]

$$Z_{eff} = \frac{\sigma_{t,a}}{\sigma_{t,el}} \tag{5}$$

The electron density can be defined as the number of electrons per unit mass, and is mathematically written as: [34]

$$N_{el} = \frac{\mu / \rho}{\sigma_{t,el}} \quad (6)$$

Materials and Methods

The bulks of the Y123, Y358 and Y3-8-11 were synthesized by using the conventional solid state reaction method. The high-purity (99.999%) of starting chemicals of Y_2O_3, $BaCO_3$ and CuO are required. All powders were mixed in the ratio of Y : Ba : Cu as 1 : 2 : 3, 3 : 5 : 8 and 3 : 8 : 11, respectively. The calcinations was react in air 950 °C for 24 h and cool down to room temperature. The calcinations process are repeated twice and intermediate grinding. The crushed powders and pressed with hydraulic machine into pellet with mold. The obtained samples was 30 mm diameter and 3 mm of thickness under 2,000 psi pressure. The final process was sintering at 950 °C for 24 h and annealed at 500 °C for 24 h under air. All samples test superconductivity phenomenal by using the Meissner effect at 77 K and all samples show the Meissner effect. The obtained the bulk samples of superconductors, The experimental arrangement is shown in Figure. 1. The source system was mounted on a composite of adjustable stands. This setup can move in the transverse direction for proper beam alignment. The ^{137}Cs radioactive source of 15 m Ci (555 MBq) strength was obtained from the Office of Atom for Peace (OAP), Thailand. The aluminium rod was used the scattering rod. The Compton scattered γ-rays were measured on a rotatable scintillator detector in the scattering plane by using the 2″ × 2″NaI(Tl) detector having an energy resolution of 8% at 662 keV (BICRON model 2M2/2), with CANBERRA photomultiplier tube base model 802-5. The optimum distance between the source and the scatterer was chosen to be 20 cm and that between the scatterer and detector, 20 cm. The spectra were recorded using a CANBERRA PC-based multi-channel analyzer (MCA). The spectrum on the MCA of detector gave instance counts in each of 1024 bins divided by voltage. We varied the angle of the scatter detector and acquire measurements on the MCA. The different angles (θ) were used to produce the different gamma rays energies.

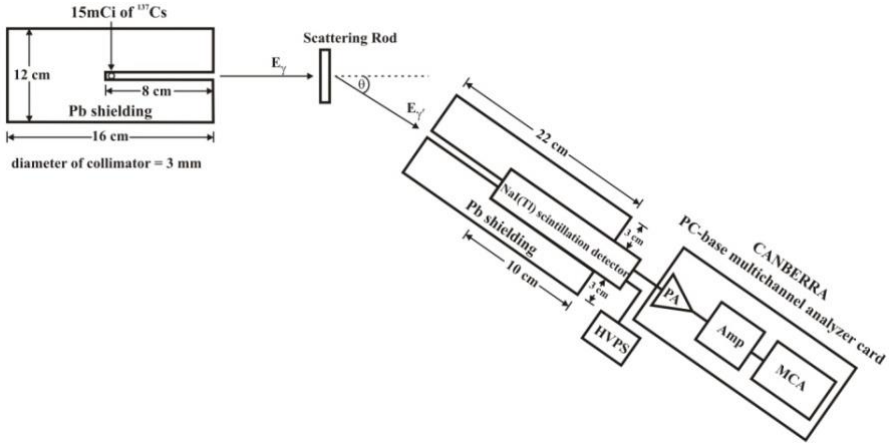

Fig. 1 Schematic of the Compton scattering experiment

An optimum sample thickness ($0.5 \leq \mu x \leq 5.0$) was selected in this experiment on the basis of the Nordforscriteria [47]. To measure mass attenuation coefficient, we placed the sample between the scattering rod and detector, and detection the acquired MCA spectra of the scattered gamma rays photo peak through sample thickness at different angles. Integrated count rates were determined from Gaussian fits and used to determine an attenuation coefficient.

The statistical error in this experiment calculated from the standard error of 3 items (i) ray-sum measurement, which calculated from experiment, the ray-sum is product of linear attenuation coefficient (μ) with thickness (x), (ii) density measurement and (iii) thickness measurement [34]. Finally, the total standard error has been determined by combining errors for the ray-sum measurement, density measurement and thickness measurement in quadrature.

Results and Discussion

The weight fractions and density of Y123, Y358 and Y3-8-11 superconductors show in Table 1. The results show the density of the samples series around 5 – 6 g cm^{-3} due to resemble in the weight fractions of constituent elements.

Table 1 The weight fractions and density of Y-based superconductors

Samples	Weight %				Density (g cm^{-3})
	Y	Ba	Cu	O	
$YBa_2Cu_3O_7$ (Y123)	7.69	15.38	23.08	53.85	4.91
$Y_3Ba_5Cu_8O_{18}$ (Y358)	8.82	14.70	23.53	52.95	5.09
$Y_3Ba_8Cu_{11}O_{24}$ (Y3-8-11)	6.52	17.39	23.91	52.18	5.19

The mass attenuation coefficients were measured at the energy range 220 – 662 keV by using Compton scattering technique for vary photon energy from Cs-137 source. The experimental values and theoretical values (obtained from WinX Com program) of the mass attenuation coefficients are show in Table 2 and variation of the mass attenuation coefficients with energy is show in Fig. 2. The result found that the mass attenuation coefficients were decrease with increasing of photon energy from 220 – 662 keV and does not show the significantly different when compared in all samples. These results are reflected to the lower of photon interaction probability at the higher photon energy. The experimental values of mass attenuation coefficient are in good agreement with the theoretical values reflecting the good detection system setup of transmission experiment and the statistical error in this experiment found to be in the range 3 – 4%.

Table 2 The mass attenuation coefficients of the samples

Energy (keV)	Y123			Y358			Y3-8-11		
	Th	Exp	%RD	Th	Exp	%RD	Th	Exp	%RD
662	7.59	7.71 ± 0.08	1.55	7.58	7.70 ± 0.08	1.51	7.59	7.70 ± 0.08	1.48
563	8.27	8.37 ± 0.17	1.20	8.26	8.30 ± 0.17	0.45	8.28	8.53 ± 0.17	3.03
482	9.01	9.16 ± 0.09	1.67	8.99	9.25 ± 0.09	2.85	9.03	9.20 ± 0.09	1.85
399	10.06	10.09 ± 0.20	0.29	10.04	10.41 ± 0.21	3.73	10.11	10.22 ± 0.20	1.08
341	11.15	11.28 ± 0.11	1.19	11.13	11.00 ± 0.11	1.21	11.25	11.40 ± 0.11	2.00
287	12.67	13.03 ± 0.26	2.81	12.64	12.70 ± 0.25	0.48	12.83	13.06 ± 0.26	1.82
253	14.14	14.24 ± 0.14	0.71	14.10	14.19 ± 0.14	0.61	14.38	14.55 ± 0.15	1.17
223	16.03	16.37 ± 0.33	2.11	15.97	16.62 ± 0.33	4.09	16.38	16.06 ± 0.32	1.92

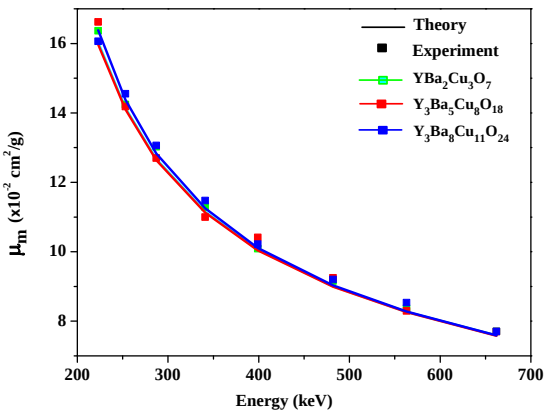

Fig. 2 The mass attenuation coefficients of the samples.

The partial interactions of Y-based superconductors calculated in the energy range 220 – 662 keV from WinX Com program as show in Table 3. The variation of partial interactions (coherent, incoherent and photoelectric) with energy is show in Fig.3 – 5 respectively. It was found that, all of partial interactions are decrease with increasing of energy in this energy range and does not show the significantly different when compared in all samples. The incoherent scattering is main interaction process. The photoelectric absorption and coherent scattering interactions were found to be small effect on attenuation process.

Table 3 The partial interactions of the samples

Energy (keV)	Coherent ($\times10^{-2}$ cm^2 g^{-1})			Incoherent ($\times10^{-2}$ cm^2 g^{-1})			Photoelectric ($\times10^{-2}$ cm^2 g^{-1})		
	Y123	Y358	Y3-8-11	Y123	Y358	Y3811	Y123	Y358	Y3-8-11
662	0.10	0.10	0.11	7.25	7.24	7.22	0.24	0.24	0.26
563	0.14	0.14	0.15	7.77	7.77	7.75	0.36	0.35	0.39
482	0.19	0.19	0.20	8.29	8.29	8.27	0.52	0.52	0.57
399	0.27	0.27	0.29	8.93	8.93	8.90	0.85	0.84	0.92
341	0.37	0.37	0.39	9.48	9.48	9.45	1.30	1.28	1.41
287	0.51	0.52	0.54	10.08	10.07	10.04	2.08	2.05	2.25
253	0.66	0.66	0.69	10.52	10.51	10.48	2.97	2.93	3.22
223	0.83	0.84	0.88	10.95	10.94	10.91	4.24	4.19	4.60

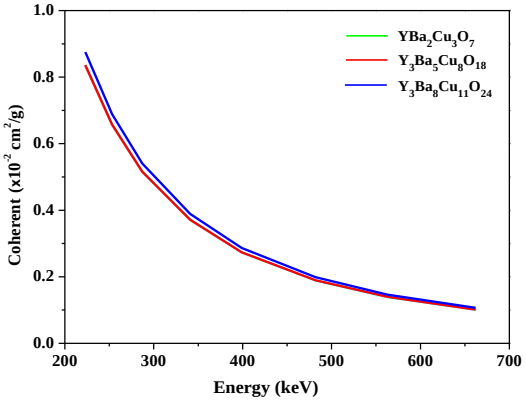

Fig. 3 The coherent scattering of the samples.

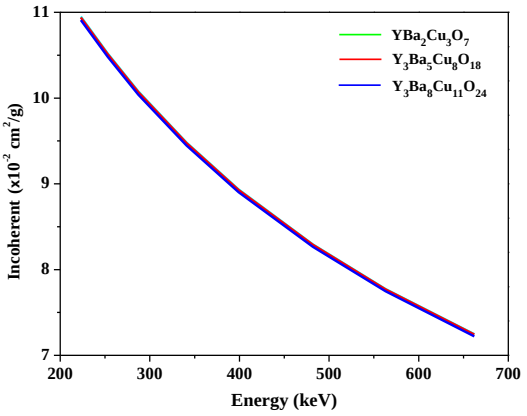

Fig. 4 The incoherent scattering of the samples.

The effective atomic numbers (Z_{eff}) were determined using equation (5). The value of effective atomic number shown in Table 4 and vary with energy show in Fig. 6. The results show that the effective atomic numbers were decrease with increasing of photon energy in this energy range. The Z_{eff} values of Y3-8-11 are highest due to the highest of Y, Ba and Cu content in all samples and found to be decrease from 13.7 e$^-$ atom^{-1} at 220 keV – 12.5 e$^-$ atom^{-1} at 662 keV.

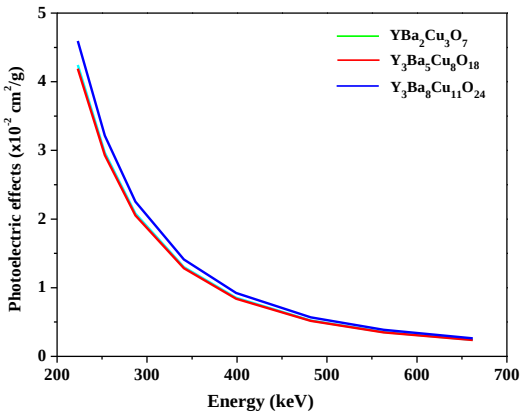

Fig. 5 The photoelectric absorption of the samples.

The Z_{eff} values of Y123 are lowest due to the lowest of Y, Ba and Cu content in all samples and found to be decrease from 13.1 e$^-$ atom^{-1} at 220 keV – 12.1 e$^-$ atom^{-1} at 662 keV. In the composite materials, the interaction (such as absorption and scattering) of gamma-rays or X-rays was related to Z_{eff} values of the composite materials and the energy of photon. The dependence on the atomic number indicates that materials having high Z_{eff} value attenuated strongly with the incoming photons.

Table 4 The effective atomic number of the samples.

Energy (keV)	Y123			Y358			Y3-8-11		
	Th	Exp	%RD	Th	Exp	%RD	Th	Exp	%RD
662	12.13	12.10 ± 0.12	0.27	12.25	12.20 ± 0.12	0.41	12.42	12.40 ± 0.12	0.16
563	12.18	12.21 ± 0.24	0.24	12.30	12.35 ± 0.25	0.45	12.48	12.50 ± 0.25	0.14
482	12.24	12.24 ± 0.12	0.01	12.36	12.40 ± 0.12	0.36	12.57	12.60 ± 0.13	0.28
399	12.35	12.39 ± 0.25	0.29	12.46	12.47 ± 0.25	0.10	12.70	12.72 ± 0.25	0.13
341	12.47	12.40 ± 0.12	0.60	12.58	12.54 ± 0.13	0.36	12.88	12.90 ± 0.13	0.15
287	12.67	12.60 ± 0.25	0.55	12.77	12.84 ± 0.26	0.48	13.13	13.15 ± 0.26	0.15
253	12.85	12.80 ± 0.13	0.41	12.95	13.03 ± 0.13	0.61	13.38	13.40 ± 0.13	0.17
223	13.08	13.16 ± 0.26	0.58	13.17	13.20 ± 0.26	0.20	13.68	13.70 ± 0.27	0.13

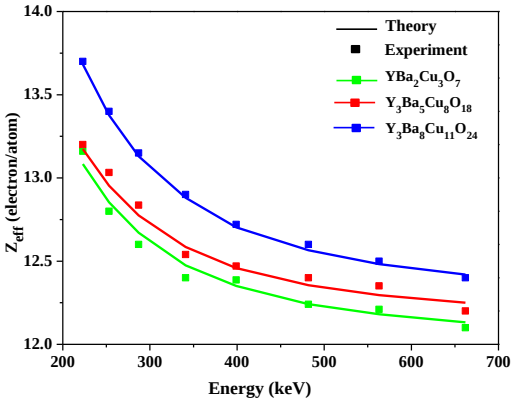

Fig. 6 The effective atomic numbers of the samples.

The variations of electron densities (N_e), i.e., the number of electron per unit mass, were shown in Table 5 and Fig. 7. The results showed that the variations of the electron densities with the gamma ray energies showed the same trend with the effective atomic numbers. Therefore, the higher values of N_e indicated the higher probability of the photon interaction in Y-based superconductors. In this work, the results clearly showed that N_e depended on the Y, Ba and Cu content in Y-based superconductors and the gamma rays energy interacted on the glasses.

Table 5 The effective atomic number of the samples.

Energy (keV)	Y123			Y358			Y3-8-11		
	Th	Exp	%RD	Th	Exp	%RD	Th	Exp	%RD
662	2.87	2.85 ± 0.02	0.68	2.87	2.87 ± 0.03	0.11	2.87	2.87 ± 0.03	0.01
563	2.88	2.89 ± 0.05	0.31	2.88	2.88 ± 0.05	0.02	2.88	2.88 ± 0.05	0.17
482	2.90	2.89 ± 0.02	0.18	2.89	2.91 ± 0.02	0.64	2.90	2.90 ± 0.02	0.14
399	2.92	2.93 ± 0.05	0.29	2.92	2.92 ± 0.05	0.15	2.94	2.93 ± 0.05	0.20
341	2.95	2.96 ± 0.03	0.32	2.95	2.95 ± 0.03	0.16	2.98	2.97 ± 0.03	0.23
287	3.00	2.99 ± 0.06	0.23	2.99	2.99 ± 0.06	0.01	3.03	3.03 ± 0.06	0.15
253	3.04	3.06 ± 0.03	0.71	3.03	3.04 ± 0.03	0.28	3.09	3.08 ± 0.03	0.38
223	3.09	3.10 ± 0.06	0.17	3.08	3.09 ± 0.06	0.23	3.16	3.16 ± 0.06	0.07

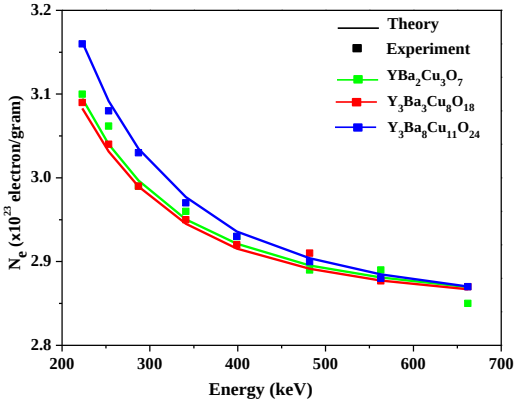

Fig. 7 The electron densities of the samples.

Conclusion

The bulks of the Y123, Y358 and Y3-8-11 were synthesized by using the conventional solid state reaction method. The calcinations and sintering were carries out in air at 950 °C for 24 h and annealed at 500 °C for 24 h in air. The densities of the samples are 4.9 – 6.0 g cm^{-3}. The mass attenuation coefficients, partial interactions and effective atomic numbers were measured and calculated at energy range of 220 – 662 keV. The mass attenuation coefficients and effective atomic numbers found to be decrease with increasing of photon energy and the incoherent scattering is the

main interaction in this energy range for all samples. The values of effective atomic numbers and electron densities are depend on Y, Ba and Cu content in the samples, highest for Y3-8-11 and lowest for Y123.

References

[1] J.G. Bednorz, K.A. Muller, Possible High T_c Superconductivity in the Ba-La-Cu-O System, Z. Phys. B. 64 (1986) 189 – 193.

[2] K. Wu, R. Ashburn, C.J. Tong, P.H. Hor, R.L. Meng, L. Gao, Z.J. Huang, Y.Q. Wang, C.W. Chu, Superconductivity at 93 K in a New Mixed-Phase Y-Ba-Cu-O Compound System at Ambient Pressure, Phys. Rev. Lett. 58 (1987) 908 – 910.

[3] P. Romano, R. Dileo, A.M. Cucola, A. Nigro, B. Dabrowski, P.G. Radaelli, Tunnel Junction on 1 : 2 : 4 Y-Ba-Cu-O Single Crystal, Physica C. 235 – 240 (1994) 1913 – 1914.

[4] P. Marsh, R.M. Fleming, M.L. Mandich, A.M. Desantolo, J. Kwo, M, Hong, L.J. Martinez-Miranda, Crystal Structure of the 80 K Superconductor $YBa_2Cu_4O_8$, Nature. 334 (1988) 141 – 143.

[5] Y. Yamada, S. Funaki, F. Nakayama, Phase control and growth of Y123 and Y124 crystals below 600 °C by molten KOH flux, Physica C. 512 (2015) 28 – 31.

[6] A. Alibadi, Y.A. Farschi, M. Akhavan, A new Y-based HTSC with Tc with above 100 K, Physica C. 469 (2009) 2012 – 2014.

[7] A. Tavana, M. Akhavan, How Tc can go above 100 K in the YBCO family, Eur. Phys. J. B. 73 (2010) 79 – 83.

[8] P. Udomsamuthirun, T. Kruaehong, T. Nilkamjon, S. Ratreng, The New Superconductors of YBaCuO Material, J. Supercond. Nov. Magn. 23 (2010) 1377 – 1380.

[9] S. Sujinnapram, P. Udomsamutthirun, T. Kruaehong, T. Nilkamjon, S. Ratreng, XRD Spectra of New YBaCuO Superconductors, Bull. Mater. Sci. 34 (2011) 1053 – 1057.

[10] H.M. Rietveld, A profile refinement method for nuclear and magnetic structures, J. Appl. Crystallogr. 2 (1969) 65 – 71.

[11] S. Kutuk, S. Bolat, C. Terzioglu, S.P. Altintas, An investigation of magnetoresistivity properties of an $Y_3Ba_5Cu_8O_y$ bulk superconductor, J. Alloy. Compound. 650 (2015) 159 – 164.

[12] C.J.V. Oliveira, A.D. Bortolozo, B. Ferreira, C.A.M. dos Santos, A.J.S. Machado, Effect of Ta_2O_5 addition on the texture of the Y123 superconductor, Physica C. 422 (2005) 83 – 87.

[13] D. Volochovan, P. Diko, M. Radusovska, V. Antal, S. Piovarci, K. Zmorayova, M. Sefcikova, Growth of Y123 bulk crystals in $Y_{1.5}Ba_2Cu_3O_x$ system with CeO_2 addition, J. Cryst. Growth. 353 (2012) 31 – 34.

[14] K. Rogacki, B. Dabrowski. Increase of critical currents in chemically substituted Y123. Physica C. 460 – 462 (2007) 406 – 407.

[15] H. Cao, N. Moutalbi, C. Harnois, R. Hua, J. Li, L. Zhou, J.G. Noudem, Novel configuration of processing bulk textured $YB_2Cu_3O_{7-x}$ superconductor by seeded infiltration growth method, Physica C. 470 (2010) 68 – 74.

[16] K. Rogacki, B. Dabrowski, Increase of critical currents in chemically substituted Y123. Physica C. 460 – 462 (2007) 406 – 407.

[17] S. Nariki, N. Sakai, M. Murakami, I. Hirabayashi, Barium cerate as effective flux pinning centers in Y123bulk materials, Physica C. 426 – 431 (2005) 602 – 607.

[18] A. Murakami, K. Katagiri, K. Kasaba, H. Miyata, Y. Shoji, Bending mechanical properties of a single-grain Y123 bulk superconductor at liquid nitrogen temperature, Physica C. 445 – 448 (2006) 361 – 365

[19] T. Nakashima , J. Shimoyama, Y. Ishii, Y. Yamazaki, H. Ogino, S. Horii, K. Kishio, True effects of microstructure and oxygen contents on flux-pinning properties of Y123 melt-solidified bulks, Physica C. 468 (2008) 1404 – 1407.

[20] F. N. Werfel, U. Floegel-Delor, T. Riedel, B. Goebel, R. Rothfeld, P. Schirrmeister, D. Wippich, Large-scale HTS bulks for magnetic application, Physica C. 484 (2013) 6 – 11.

[21] Y.H. Han, J-S. Lee, T-H. Sung, S-C. Han, Y-C. Kim, S-J. Kim, Design a hybrid High T_c superconductor bearings for flywheel energy storage system, Physica C. 372 – 376 (2002) 1457 – 1461.

[22] N. Koshizuka, F. Ishikawa, H. Nasu, M. Murakami, K. Matsunaga, S. Saito, O. Saito, Y. Nakamura, H. Yamamoto, R. Takahata, Y. Itoh, H. Ikezawa, M. Tomita, Progress of superconducting bearing technologies for flywheel energy storage systems, Physica C. 386 (2003) 444 – 450.

[23] T. Tsuchiya, T. Kikuchi, S. Takano, N. Koshizuka, M. Murakami, Effect of magnetic particle additions on flux pinning in bulk Y-Ba-Cu-O superconductors, Phys. Procedia. 27 (2012) 156 – 159.

[24] A. Un, F. Demir, Determination of mass attenuation coefficients, effective atomic numbers and effective electron numbers for heavy-weight and normal-weight concretes, Appl. Radiat. Isotopes. 80 (2013) 73 – 77.

[25] I. Akkurt, H. Akyıldırım, F. Karipçin, B. Mavi, Chemical corrosion on gamma-ray attenuation properties of barite concrete, J. Saudi Chem. Soc. 16 (2012) 199 – 202.

[26] I. Akkurt, R. Altindag, K. Gunoglu, H. Sarıkaya, Photon attenuation coefficients of concrete including marble aggregates, Ann. Nucl. Energy. 43 (2012) 56 – 60.

[27] J. Kaewkhao, J. Laopaiboon, W. Chewpraditkul, Determination of Effective Atomic Numbers and Effective Electron Densities of Cu/Zn Alloy, J. Quant. Spectrosc. Ra. 109 (2008) 1260 – 1265.

[28] P. Limkitjaroenporn, J. Kaewkhao, W. Chewpraditkul, P. Limsuwan, Mass Attenuation Coefficient and Effective Atomic Number of Ag/Cu/Zn Alloy at Different Photon Energy by Compton Scattering Technique, Procedia Eng. 32 (2012) 847 – 854.

[29] P. Limkitjaroenporn, J. Kaewkhao, S. Asavavisithchai, Determination of mass attenuation coefficients and effective atomic numbers for Inconel 738 alloy for different energies obtained from Compton scattering, Ann. Nucl. Energy. 53 (2012) 64 – 68.

[30] V.P. Singh, N.M. Badige, Gamma ray and neutron shielding properties of some alloy materials, Ann. Nucl. Energy. 64 (2014) 301 – 310.

[31] I. Akkurt, A. Calik, H. Akyıldırım, Theboronizing effect on the radiation shielding and magnetization properties of AISI 316L austenitic stainless steel, Nucl. Eng. Des. 241 (2011) 55 – 58.

[32] P. Limkitjaroenporn, J. Kaewkhao, Gamma-rays attenuation of zircons from Cambodia and South Africa at different energies: A new technique for identifying the origin of gemstone, Radiat. Phys. Chem. 103 (2014) 67 – 71.

[33] T. Korkut, H. Korkut, A. Karabulut, G. Budak, A new radiation shielding material: Amethyst ore, Ann. Nucl. Energy. 38 (2011) 56 – 59.

[34] P. Limkitjaroenporn, J. Kaewkhao, P. Limsuwan, W. Chewpraditkul, Physical, optical, structural and gamma-ray shielding properties of lead sodium borate glasses, J. Phys. Chem. Solids. 72 (2011) 245 – 251.

[35] S. Kaewjaeng, J. Kaewkhao, P. Limsuwan, U. Maghanemi, Effect of BaO on Optical, Physical and Radiation Shielding Properties of SiO_2-B_2O_3-Al_2O_3-CaO-Na_2O Glasses System, Procedia Eng. 32 (2012) 1080 – 1086.

[36] K. Kirdsiri, J. Kaewkhao, N. Chanthima, P. Limsuwan, Comparative study of silicate glasses containing Bi_2O_3, PbO and BaO: Radiation shielding and optical properties, Ann. Nucl. Energy. 38 (2011) 1438 – 1441.

[37] K.J. Singh, S. Kaur, R.S. Kaundal, Comparative study of gamma ray shielding and some properties of PbO-SiO_2-Al_2O_3 and Bi_2O_3-SiO_2-Al_2O_3 glass systems, Radiat. Phys. Chem. 96 (2014) 153 – 157.

[38] M.H. Kharita, R. Jabra, S. Yousef, T. Samaan, Shielding properties of lead and barium phosphate glasses, Radiat. Phys. Chem. 81 (2012) 1568 – 1571.

[39] K. Singh, H. Singh, V. Sharma, R. Nathuram, A. Khanna, R. Kumar, S.S. Bhatti, H.S. Sahota, Gamma-Ray Attenuation Coefficients in Bismuth Borate Glasses, Nucl. Instrum. Meth. B. 194 (2002) 1 – 6.

[40] K.S. Mann, A. Rani, M.S. Heer, Shielding behaviors of some polymer and plastic materials for gamma-rays, Radiat. Phys. Chem. 106 (2015) 247 – 254.

[41] V.P. Singh, S.P. Shirmardi, M.E. Medhat, N.M. Badiger, Determination of mass attenuation coefficient for some polymers using Monte Carlo simulation, Vacuum. 119 (2015) 284 – 288.

[42] H. Baltaş, U. Çevik, E. Tıraşoğlu, B. Ertuğral, G. Apaydın, A.İ. Kobya, Mass attenuation coefficients of YBaCuO and BiPbSrCaCuO superconductors at 511, 661 and 1274 keV energies, Radiat. Meas. 39 (2005) 33 – 37.

[43] H. Baltaş, Ş. Çelik, U. Çevik, E. Yanma, Measurement of mass attenuation coefficients and effective atomic numbers for MgB_2 superconductor using X-ray energies, Radiat. Meas. 42 (2007) 55 – 60.

[44] U. Çevik, H. Baltaş, Measurement of the mass attenuation coefficients and electron densities for BiPbSrCaCuO superconductor at different energies, Nucl. Instrum. Meth. B. 256 (2007) 619 – 625.

[45] L. Gerward, N. Guilbert, K.B. Jensen, H. Levring, X-ray absorption in matter. Reengineering XCOM, Radiat. Phys. Chem. 60 (2001) 23 – 24.

[46] L. Gerward, N. Guilbert, K.B. Jensen, H. Levring, WinXCom-a program for calculation X-ray attenuation coefficients, Radiat. Phys. Chem. 71 (2004) 653 – 654.
[47] B. Nordfors, The statistical error in X-ray absorption measurements, ArkivfoerFysik. 18 (1960) 37 – 47.